Published in final edited form as:
Clin Cancer Res. 2012 March 1; 18(5): 1268–1280. doi:10.1158/1078-0432.CCR-11-1795.

Telomestatin Impairs Glioma Stem Cell Survival and Growth through the Disruption of Telomeric G-Quadruplex and Inhibition of the Proto-oncogene, *c-Myb*

Takeshi Miyazaki[1], **Yang Pan**[1], **Kaushal Joshi**[1], **Deepti Purohit**[1], **Bin Hu**[1], **Habibe Demir**[1], **Sarmistha Mazumder**[1], **Sachiko Okabe**[2], **Takao Yamori**[3], **Mariano Viapiano**[1], **Kazuo Shinya**[4], **Hiroyuki Seimiya**[2], and **Ichiro Nakano**[1]

[1]Department of Neurological Surgery, Dardinger, Center for Neuro-oncology, James Cancer Hospital and The Ohio State University, Columbus, Ohio

[2]Division of Molecular Biotherapy, Tokyo, Japan

[3]Division of Molecular Pharmacology, Cancer Chemotherapy, Center of Japanese Foundation for Cancer Research, Tokyo, Japan

[4]National Institute of Advanced Industrial Science and Technology, Tokyo, Japan

Abstract

Purpose—Glioma stem cells (GSC) are a critical therapeutic target of glioblastoma multiforme (GBM).

Experimental Design—The effects of a G-quadruplex ligand, telomestatin, were evaluated using patient-derived GSCs, non-stem tumor cells (non-GSC), and normal fetal neural precursors *in vitro* and *in vivo*. The molecular targets of telomestatin were determined by immunofluorescence *in situ* hybridization (iFISH) and cDNA microarray. The data were then validated by *in vitro* and *in vivo* functional assays, as well as by immunohistochemistry against 90 clinical samples.

Results—Telomestatin impaired the maintenance of GSC stem cell state by inducing apoptosis *in vitro* and *in vivo*. The migration potential of GSCs was also impaired by telomestatin treatment. In contrast, both normal neural precursors and non-GSCs were relatively resistant to telomestatin. Treatment of GSC-derived mouse intracranial tumors reduced tumor sizes *in vivo* without a noticeable cell death in normal brains. iFISH revealed both telomeric and non-telomeric DNA damage by telomestatin in GSCs but not in non-GSCs. cDNA microarray identified a proto-oncogene, *c-Myb*, as a novel molecular target of telomestatin in GSCs, and pharmacodynamic analysis in telomestatin-treated tumor-bearing mouse brains showed a reduction of *c-Myb* in tumors *in vivo*. Knockdown of *c-Myb* phenocopied telomestatin-treated GSCs both *in vitro* and *in vivo*, and restoring *c-Myb* by overexpression partially rescued the phenotype. Finally, *c-Myb* expression was markedly elevated in surgical specimens of GBMs compared with normal tissues.

Corresponding Author: Ichiro Nakano, Ohio State University, 385A Wiseman Hall, 410 W 12th St., Columbus, OH 43210. Phone: 614-292-0358; Fax: 614-688-4882; Ichiro.Nakano@osumc.edu.

Note: Supplementary data for this article are available at Clinical Cancer Research Online (http://clincancerres.aacrjournals.org/).

Disclosure of Potential Conflicts of Interest
All authors have seen and approved the manuscript. No potential conflicts of interest were disclosed.

Conclusions—These data indicate that telomestatin potently eradicates GSCs through telomere disruption and *c-Myb* inhibition, and this study suggests a novel GSC-directed therapeutic strategy for GBMs.

Introduction

The development of effective therapies for glioblastoma multiforme (GBM) is a challenging endeavor due to the aggressive proliferation and the high migratory potential of this form of cancer. Recent studies have suggested the existence of a hierarchical organization of multiple heterogeneous cell populations in GBMs having distinct tumordriving capacities (1). Among heterogeneous tumor cells, glioma stem cells (GSC) are defined as a subpopulation that is capable of self-renewal and differentiation into multi-lineaged tumor cells with distinct tumorigenic potentials *in vivo*. The resistance of GSCs to current forms of therapy is likely related to the failure of current treatments (2). Identification of novel therapeutic strategies for GSCs in GBMs remains a major hurdle to effectively attack this highly malignant tumor. GSCs exhibit phenotypic and genetic similarities to their somatic counterparts, neural stem cells (NSC). Targeting shared pathways that regulate the survival of both GSCs and NSCs, therefore, may eradicate both types of stem cells. To accomplish the selective targeting of GSCs over NSCs, it is crucial to uncover the mechanisms that specifically regulate the initiation of GBMs and the maintenance of the stem cell–like phenotype of GSCs.

Human chromosomes are capped with telomeres, regions of repeating DNA that prevent the degradation of genes at the chromosomal ends (3). Because of incomplete replication of linear DNA ends, human somatic cells progressively shorten their telomeres during every round of cell division. Immortalized cancer cells have an increased ability to extend their telomeres, which is one of the reasons that cancer cells can bypass replication senescence and subsequent cell death (4, 5). If indefinite cell division is a property that is unique to tumor stem cells, one potential approach to target GSCs would be to disrupt telomere extension. In the process of telomere elongation, the enzyme telomerase plays a critical role. Despite the emerging hope for attacking telomerase in cancers based on this unique character, the major limitation of this approach in clinical settings is its delayed effectiveness.

Telomestatin is a natural product isolated from *Streptomyces anulatus* 3533-SV4 (6) and stabilizes the G-quadruplex (7) that is postulated to be present in telomeric DNA (3) and in the promoter regions of several proto-oncogenes (8–11). Formed G-quadruplex structures function as transcriptional repressor elements (12). Treatment with telomestatin induces apoptosis of various cancer cells with relatively less of an effect on somatic cells (13, 14). Although the effect of telomestatin on telomeric DNA has been well described, it is not clear whether it is the only mechanism of higher sensitivity of cancer cells over somatic cells. In addition, the sensitivity of cancer stem cells to telomestatin has not been shown yet.

Here, we show that telomestatin triggers the preferential apoptosis of GSCs with less of an effect on normal precursors or non-GSCs in GBMs. Immunofluorescence *in situ* hybridization (iFISH) detected the presence of damage in both telomeric and non-telomeric DNA regions in GSCs but not in non-GSCs. Analysis of a cDNA microarray identified a reduction in the proto-oncogene, *c-Myb*, following telomestatin treatment of GSCs. Decreased *c-Myb* expression was also observed in pharmacodynamic analyses of telomestatin-treated xenografted tumors. Moreover, treatment of tumor-bearing mice showed a statistically significant reduction in tumor sizes *in vivo*. Finally, immunohistochemistry of clinical samples of GBMs and normal tissues exhibited a statistically significant elevation of c-Myb levels in tumors. Collectively, these data suggest

that targeting GSCs with telomestatin has the potent effect on diminishing GBM growth *in vitro* and *in vivo* through disruption of telomeric DNA and inhibition of *c-Myb*.

Materials and Methods

Cell lines and cell culture

Characteristics of 8 GBMs (GBM146, 157, 205, 206, 218, 1600, 2313, and 13) and 2 non-tumor human fetal brain specimens (f16w and 1105A) from aborted fetus were published previously (15–18). Methods for establishment of GBM sphere cultures and normal sphere cultures are published previously (16, 18) and details are described in Supplementary Information. All the experiments were carried out with short-term cultures within 20 passages.

Chemicals

Telomestatin was synthesized in the Biomedicinal Information Research Center, National Institute of Advanced Industrial Science and Technology (Tokyo, Japan). The quality of telomestatin was assessed with HPLC (UPLC) system and the readout was based on the UV absorptions. The structure of telomestatin was also confirmed by ^{1}H and ^{13}C NMR spectra. Other anticancer drugs and chemicals were purchased from Sigma-Aldrich and dissolved in dimethyl sulfoxide (DMSO).

Flow cytometric analysis, fluorescence-activated cell sorting, sphere-forming assay, immunostaining, apoptosis assay, cell growth assay, xenograft, Western blot analysis, tumor size measurement, iFISH assay, transient transfection, lentivirus-mediated short hairpin RNA, and reverse transcriptase PCR

Detailed methods are published previously (16, 18–20) and described in Supplementary Information.

Brain slice invasion assay

Brain slice invasion assay was conducted as described previously (21). Briefly, GBM spheres of 300 to 400 μm diameter were treated with telomestatin or vehicle (DMSO) for 24 hours. Coronal brain slices obtained from neonatal mice were prepared for organotypic culture. Viable spheres that did not stain with propidium iodide were washed in slice medium, manually placed on the brain slices, and imaged by fluorescence microscopy every 24 hours. Cells from spheres treated with telomestatin were also assessed for cell viability using an assay for reduction of soluble tetrazolium (Cell Titer kit, Promega).

cDNA microarray

RNA was extracted from GBM sphere samples treated with DMSO or 1 μmol/L telomestatin for 24 hours with RNeasy Mini Kit following the manufacturer's protocol (QIAGEN). RNA samples were analyzed by the FGC using an Agilent 2100 Bioanalyzer Lab-On-A-Chip Agilent 6000 Series II chip to determine the integrity of the samples. Sample labeling and hybridization were conducted according to the manufacturer's protocols.

Scanning and image analysis—Microarray slides were hybridized overnight, washed, and then scanned with Agilent G2505C Microarray Scanner. The information about each probe on the array was extracted from the image data using Agilent Feature Extraction 10.5 (FE). The raw intensity values from these files are imported into the mathematical software package "R," which is used for all data input, diagnostic plots, normalization, and quality checking steps of the analysis process.

Tissue microarray

The slides of GBM tissue microarray were obtained from Department of Pathology at the Ohio State University (OSU; Columbus, OH). After deparaffinization by xylene, immunohistochemistry with the c-Myb antibody was carried out as described previously (22). Isogenic IgG control was used to confirm the specific signals for c-Myb immunoreactivity. The staining intensities were blindly categorized into 3 groups (negative, single positive, double positive) by 2 independent neuropathologists.

Statistics

Values are given as means ± SD, unless noted otherwise in the figure legend. The number of replicates is noted in the figure or legends. Absent error bars in the bar graphs signify that SD values are smaller than the graphic symbols. Comparison of mean values between multiple groups was evaluated by a Tukey honestly significant difference (HSD) test for post-ANOVA pairwise comparisons in a one-way ANOVA unless noted otherwise in the figure legend. Comparison of mean values between 2 groups was evaluated by χ^2 test or Student *t* test. All statistical tests were two-sided. For all statistical methods, a *P* value less than 0.05 was considered significant.

Results

Telomestatin is a relatively selective inhibitor of brain tumor cell lines and inhibits growth of patient-derived GBM spheres *in vitro*

The effect of telomestatin *in vitro* was first tested on a panel of 39 human cancer cell lines (JFCR39; Fig. 1A; ref. 23). Cells derived from tumors of the central nervous system (CNS) exhibited higher sensitivity than others. With these brain tumor cell lines, the concentration of telomestatin required for a 50% growth inhibition (GI_{50}; concentration needed to reduce the growth of treated cells to half that of untreated cells) ranged between 1 and 10 μmol/L (Supplementary Fig. S1A). With patient-derived short-term GBM cell cultures (GBM1600 and 2313) propagated in serum-containing medium, the GI_{50} value was approximately 5 μmol/L (Supplementary Fig. S1B). This result suggests that telomestatin is a relatively potent and selective inhibitor of brain tumor–derived cells compared with other cancer-derived cells. Next, the sensitivity of GSCs to telomestatin was examined. Sphere-forming potential is one unique characteristic of GSCs (24, 25). Using short-term cultures derived from specimens of 5 patients with GBMs, we investigated the effect of varying doses of telomestatin on sphere formation (Supplementary Fig. S1C). Remarkably, in all samples, treatment with 1 μmol/L telomestatin completely abolished sphere formation. In 3 of these 5 samples, treatment with 0.1 μmol/L of telomestatin significantly reduced sphere numbers as well ($P < 0.05$; Supplementary Fig. S1C). These results suggest a prominent inhibitory effect of telomestatin on GSC phenotypic sphere formation capability *in vitro*.

Telomestatin preferentially inhibits survival of patient-derived GSCs compared with normal neural precursor cells

In several organs, a differential sensitivity to telomestatin treatment was previously observed between tumor cells and their somatic counterparts (13, 14). We therefore sought to compare the effects of telomestatin treatment on the growth of patient-derived GSCs and normal neural precursors derived from human fetal brains. Normal neural precursors and GSCs were enriched in serum-free media with the supplement of basic fibroblast growth factor and epidermal growth factor (Supplementary Fig. S2). When both of these cultures were stimulated with 10% FBS for differentiation, multiple types of lineage-committed cells were observed, as seen by a decline in Sox2 expression and upregulation of neuron-specific class III β-tubulin (TuJ1) and glial fibrillary acid protein (GFAP; Supplementary Fig. S2).

Following examination of these precursor cells, we found that compared with GSCs, neural precursor cells were relatively resistant to telomestatin treatment (Fig. 1B). The graph in Fig. 1B shows a significant difference of relative cell numbers between 3 GSC samples (GBM146, 157, and 206) and 2 normal neural precursor samples (f16w and 1105A) after treatment with 1 μmol/L telomestatin for 96 hours. These data suggest that telomestatin treatment strongly impairs GSC growth, whereas normal neural precursors are less sensitive to telomestatin treatment. Likewise, we verified the effective dose of telomestatin required to affect the growth properties of human astrocyte primary cultures and immortalized human astrocytes overexpressing *E6*, *E7*, and *hTERT* (normal human astrocytes; NHA). One phenotypic difference between these two cultures is that only NHA cells are tumorigenic in immunocompromised mouse brains (26). Following incubation of these 2 cultures with varying doses of telomestatin for 96 hours, we found that normal astrocytes are more resistant to treatment than NHA cultures (Supplementary Fig. S1D).

A cell surface protein, CD133, is not a universal marker for GSCs in GBMs (27); however, we have found that in some of our clinical samples, positive CD133 expression correlates well with properties of GSCs, including tumorigenicity, *in vitro* clonogenic potential, multilineage differentiation capability, and high expression of stem cell–related genes and proteins (15, 18). We therefore reasoned that if telomestatin preferentially eradicates GSCs, the proportion of CD133-positive cells among total GBM cells should decrease with treatment. To explore this possibility, we treated tumor spheres derived from the 3 GBM cases with varying doses of telomestatin for 48 hours and conducted fluorescence-activated cell sorting (FACS) to determine the proportion of CD133-positive cells. As expected, telomestatin treatment reduced the proportion of CD133-positive cells in a dose-dependent manner with the proportion of CD133-positive cells being approximately half of the control samples at 1 μmol/L concentration (91.5% vs. 62.2% in GBM146, 92.6% vs.43.5% in GBM157, and 60.7% vs. 24.3% in GBM206; Fig. 1C, top, and Supplementary Fig. S3A). By separation of GBM157 cells based on cell surface CD133 expression, we confirmed that sphere-forming potential is restricted to CD133-positive cells, but not CD133-negative, cells (Supplementary Fig. S3B). When treated with telomestatin (1 μmol/L), these sphere-forming cells were eliminated (Supplementary Fig. S3B). Immunocytochemistry with a CD133 antibody and Hoechst dye showed that telomestatin treatment resulted in the condensed fragmentation of nuclei of CD133-positive cells, suggesting the induction of apoptosis, but not differentiation of CD133-positive cells into CD133-negative cells by telomestatin (Fig. 1C, bottom). Taken together, these results show that telomestatin treatment preferentially eradicates GSCs through an apoptotic mechanism.

We then sought to determine the effect of telomestatin on GSC self-renewal. One means of estimating *in vitro* self-renewal is through the use of serial assays to test multiple rounds of sphere-forming capacity (28). We analyzed the capacity of these cells to form secondary spheres after telomestatin treatment (Fig. 1D). Following 7 days of incubation with telomestatin, we carried out secondary sphere-forming assays using drug-free culture conditions. A reduction in secondary sphere numbers was observed with even less concentrations of telomestatin (0.2–0.5 μmol/L), indicating that treatment with lower doses of telomestatin abolishes self-renewal capacity of GSCs *in vitro*.

Treating tumor-bearing mice with telomestatin reduces tumor growth *in vivo*

We next sought to test the effect of telomestatin treatment on tumor cell growth *in vivo*. First, we conducted transplantation of 2 GBM sphere samples (GBM146 and 157) pretreated with telomestatin (1 or 5 μmol/L) into immunocompromised mouse brains in accordance with Institutional Animal Care and Use Committee–approved protocols at OSU (Supplementary Fig. S4). These tumor-bearing mice were then sacrificed at 3 months

posttransplantation, and sizes of resultant tumors were determined by immunohistochemistry with human-specific nestin and vimentin antibodies. The average size of intracranial tumors was reduced with the lower dose (1 μmol/L; Supplementary Fig. S4B and S4E) and almost completely abolished with the higher dose (5 μmol/L) of telomestatin (Supplementary Fig. S4C and S4F). Similar results were observed with the GBM146-derived model treated with 5 μmol/L telomestatin (Supplementary Fig. S4D and S4G). Collectively, pretreatment of GSCs with telomestatin potently inhibits their *in vivo* tumor formation and growth.

Second, we evaluated the therapeutic efficacy of telomestatin by injection into the intracranial tumor cavities of immunocompromised mice. The mouse intracranial tumors were created by implantation of GBM157 spheres into the striatum (Fig. 2A). We then injected telomestatin at 2 different time points; at day 0 (on the day of tumor implantation) and at day 14. The rationale for choosing these 2 time points is to investigate separately the effect of telomestatin on both tumor initiation and growth of established tumors. We then measured tumor sizes 3 months after transplantation. The effect of the treatment was evaluated by immunohistochemistry using a human-specific nestin antibody and a vimentin antibody (Fig. 2B; ref. 18). In both cases, local injection of telomestatin resulted in a 55% to 71% reduction in the overall tumor size, determined by nestin immunoreactivity (Fig. 2B, top). Similarly, a 72% to 76% reduction was observed with vimentin staining (Fig. 2B, bottom). To verify whether this procedure produces any cytotoxic effects on normal brain, we conducted immunohistochemistry for activated caspase-3, a marker for apoptosis, in mouse brains bearing tumor cells 2 days after telomestatin injection. Activated caspase-3 immunoreactivity was strictly restricted within the telomestatin-injected tumor lesions and not in adjacent normal brain tissues including the subventricular zone of the lateral ventricles (Fig. 2C, top). These data were in concurrence with the results of Ki-67 staining which shows a reduction in proliferating cells in telomestatin-treated tumors (Fig. 2C, bottom left). In control tumors treated with DMSO, few cells were positive for activated caspase-3, even in the area of tumor cell injection (Fig. 2C, bottom right). In summary, we confirmed that intratumoral telomestatin treatment significantly diminishes tumor size *in vivo* without causing the apparent death of normal cells.

Telomestatin reduces migration of GSCs *in vitro* and *in vivo*

One of the hallmarks of human GBMs is its invasive and infiltrative nature. In agreement with recent studies that showed an enhanced ability of GSCs for migration and invasion (29), GSC-derived tumor models exhibit aggressive migration upon transplantation into mouse brains (Fig. 3A). Of note, telomestatin-treated tumor cells showed significantly less migration into the contralateral hemisphere (Fig. 3A, bottom). This could be due to a reduced number of live tumor cells and/or reduced invasive capacity. To further study this observation, we conducted an assay for cell invasion on organotypic cultures of brain tissue which mimics brain cytoarchitecture and natural barriers to cell movement (Fig. 3B; ref. 21). First, we confirmed that undifferentiated GBM spheres (GSC) possess greater migration potential into mouse brains than non-GSCs from the same samples (Fig. 3C). We then treated GBM146 and 157 spheres with 3 different doses of telomestatin for 24 hours, seeded them onto mouse brain slices, and used fluorescence microscopy to evaluate invasion for up to 72 hours, as previously described (30). Both GBM sphere samples dispersed aggressively through brain tissue in the absence of the drug (Fig. 3D). In contrast, telomestatin significantly reduced cell migration in a concentration-dependent manner. Assessment of viability by *in situ* fluorescence and parallel viability assays indicated that this effect was specific for cell migration; as telomestatin did not affect viability of nondissociated spheres until 48 hours (5 μmol/L) to 96 hours (1 μmol/L) after treatment (data not shown).

Collectively, these data indicate that telomestatin abrogates both growth and migration of GSCs *in vivo* and *in vitro*.

Telomestatin-treated GSCs, but not non-GSCs, undergo apoptosis through both telomeric and non-telomeric DNA damage

Although previous studies have reported several different mechanisms of action for telomestatin, it appears to kill non-CNS tumor cells primarily through DNA damage–derived apoptosis (13, 14, 31–33). When GBM sphere samples (GBM146, 157, and 206) were treated with telomestatin, we found a 17% to 35%increase in the number of cells with fragmented nuclei by Hoechst dye staining, a typical morphologic feature of apoptotic cell death (Fig. 4A). An abundance of apoptotic cells in telomestatin-treated GBM146 and 157 spheres was also confirmed by staining with fluorescein-conjugated Annexin V antibody and labeling with propidium iodide (Supplementary Fig. S5A). Western blot analysis showed an induction of p53 in telomestatin-treated GBM spheres (Supplementary Fig. S5B).

Because our data in Fig. 1 suggest that the potency of telomestatin is predominant in CNS tumor–derived cell lines and GBM spheres, we hypothesized that telomestatin has previously uncharacterized molecular targets in the non-telomeric DNA of GBM cells. To address this question, we conducted the iFISH assay that enables the simultaneous localization of telomeres and 53BP1, a marker of the DNA damage response (34). As shown in Fig. 4B, DMSO-treated control GBM146 GSCs exhibited uniform distribution of 53BP1 in the nucleoplasm, indicating that these cells did not initiate the DNA damage response under normal growth conditions. Conversely, telomestatin-treated GSCs rapidly developed punctate, nuclear 53BP1 foci in a dose-dependent manner (Fig. 4B). Importantly, some of these foci colocalized with non-telomeric DNA (Fig. 4C), therefore representing both telomeric and non-telomeric dysfunction-induced foci, a hallmark of deprotected DNA damage (35, 36). Meanwhile, consistent with their lower susceptibility to telomestatin-induced apoptosis, non-GSCs in GBM146 did not exhibit the 53BP1 foci upon treatment with telomestatin or DMSO under the identical culture condition (Fig. 3B and data not shown). Taken together, these results indicate that telomestatin induces telomeric and non-telomeric DNA damage preferentially in GSCs, and the loss of tumor *stemness* is likely associated with a failure in the DNA damage response in GSCs elicited by telomestatin.

c-Myb is another target of telomestatin in GSCs

The presence of 53BP1 foci in DNA regions separate from telomeres led us to search for target genes of telomestatin. To this end, we carried out cDNA microarray experiments using 4 GBM sphere samples with or without telomestatin treatment. Specifically, we focused on changes in G-quadruplex–interacting genes and telomere-related genes. Among the 15 genes identified, only c-Myb expression was significantly decreased in all 4 telomestatin-treated GBM sphere samples (Fig. 5A). An analysis of genes that were previously reported as *stemness*-related genes or proneuronal, mesenchymal, or proliferative GBMs (36) did not identify any gene whose expression was significantly decreased by telomestatin treatment (Fig. 5A). Downregulation of *c-Myb* in GBM spheres was further validated by reverse transcriptase PCR (RT-PCR) and Western blot analysis in all 4 samples (Fig. 5B and Supplementary Fig. S6). Conversely, *c-Myb* expression was not affected in telomestatin-treated non-GSCs or normal precursors, and as expected, the basal levels of *c-Myb* expression in these cell populations were substantially lower than those in GSCs (Fig. 5B). Immunocytochemistry showed the presence of c-Myb expressing cells in nestin-positive GBM157 spheres (Fig. 5C, left) and the decline in c-Myb expression in telomestatin-treated GBM spheres was also confirmed by immunocytochemistry (Fig. 5C, right). In agreement with decreased expression *in vitro*, pharmacodynamic evaluation of mouse intracranial tumors at day 2 following telomestatin injection showed an *in vivo*

reduction of c-Myb immunoreactivity (Fig. 5D). These data support the idea that *c-Myb* is another molecular target of telomestatin and suggest that c-Myb is involved in survival and/or growth of GSCs in GBMs.

c-Myb regulates GSC growth *in vitro* and *in vivo*

We then sought to determine the functional role of c-Myb in GSCs both *in vitro* and *in vivo*. First, we evaluated the effect of *c-Myb* overexpression and knockdown with GBM157 spheres *in vitro*. *c-Myb* knockdown resulted in abrogated growth of GBM157 sphere cells, which phenocopied the results with telomestatin treatment (Fig. 6A, left, and Supplementary Fig. S7). In turn, c-Myb overexpression in telomestatin-treated GBM157 spheres resulted in a full recovery of sphere cell growth at 0.5 μmol/L of telomestatin and a partial recovery at 1 μmol/L of telomestatin (Fig. 6A, right, and Supplementary Fig. S7). Next, we evaluated the effect of *c-Myb* knockdown on *in vivo* tumor growth. To this end, another short-term GBM sphere culture, GBM13, was infected with lentivirus harboring short hairpin RNA for either *c-Myb* or a nontargeting sequence (Supplementary Fig. S7; ref. 26), and the survival periods of tumor-burdened mice were determined (Fig. 6B). Consequently, lentivirus-derived *c-Myb* knockdown prolonged the survival of mice with GSC-derived intracranial tumors in a statistically significant manner. Taken together, these data suggest that c-Myb plays an essential role in GSCs growth *in vitro* and *in vivo* and is a target of telomestatin in GSCs.

c-Myb is highly expressed in some GBM tissues

To evaluate the clinical relevance of the function of c-Myb in GBMs, we investigated the expression of c-Myb in 66 surgical specimens of GBMs and 24 normal brain tissues (Fig. 6C). We conducted immunohistochemical staining with these samples using an antibody for c-Myb (22). c-Myb immunoreactivity was specifically observed in the nuclear compartments in both samples. Representative pictures display the typical pattern of the staining (Fig. 6C). As a result, c-Myb was abundantly expressed in nuclei of GBM cells in 62% of samples, whereas only 25% of normal brains showed positivity of c-Myb immunoreactivity (Fig. 6D; $P = 0.004$).

Discussion

The cancer stem cell hypothesis postulates the existence of a subpopulation of poorly differentiated tumor cells with the capacity to self-renew and repopulate a diversity of lineage-committed tumor cells. By definition, *in vivo* tumor formation in immunocompromised mouse brains is the only direct evidence for the presence of GSCs within a pool of heterogeneous tumor cells. However, it is possible that this assay may select for tumor cells that have escaped from the immune system and/or human cells that have adapted to the microenvironment in mouse brains. These issues aside, the therapeutic significance of telomestatin treatment for human GBMs is suggested by its effect on *in vivo* growth in mouse brains (Fig. 2). To obtain clinically relevant data concerning the effect of telomestatin treatment, we conducted intratumoral injection of telomestatin. As a result, tumor size was significantly decreased. However, this treatment did not completely eliminate the tumors. It is possible that GSCs may contain a subpopulation of telomestatin-resistant cells. The relatively small number of samples tested in this study has allowed only limited interpretation concerning the genetic and phenotypic differences of GSCs as well as how universally effective telomestatin treatment would be on human patients with GBMs. To determine the therapeutic window of telomestatin, we need to address the question of whether or not the normal brain can tolerate doses of telomestatin required to kill tumor cells.

The cell-sorting technique using cell surface markers is one potential means of isolating stem cells. This method has been widely adopted to determine the presence of GSCs in heterogeneous tumor cells (18, 24, 25). One of the limitations of this assay is the lack of universal and definitive markers for GSCs. CD133 is the most common antigen and AC133 is a monoclonal antibody against this cell surface protein (24). This antibody appears to correlate to some extent with the presence of GSCs in multiple different cell populations (24, 37, 38). However, several studies have reported the presence of CD133-negative GSCs in GBM samples possibly due to patient-to-patient phenotypic and genetic differences (27). More recently, CD15 has gained attention as another potential marker for GSCs (38). At this point, any of the currently available cell surface antibodies are only surrogate markers for GSCs and need to be tested on a case-by-case basis. In the samples of this study, CD133, but not CD15, correlated with enrichment of GSCs (data not shown).

Telomestatin interacts with the G-quadruplex recognizing sequences in the genome which are present in the telomeric DNA (3), as well as the promoter regions of several proto-oncogenes (8–11). Previous studies have identified several potential target molecules including *hTERT* (13, 32), *c-Myc* (10), *HIF1-α* (11), *RET* (8), and platelet-derived growth factor receptor (*PDGFR*)-β (9). The effective doses found in most of these studies were relatively high, from around the several micromolar range. In this study, patient-derived GBM sphere cells underwent apoptosis at approximately 0.5 to 1 μmol/L, and no obvious change in expression of the above genes was detected. Instead, *c-Myb*, which also has the telomestatin-binding sequences in its promoter region (39), was the only gene showing a significant reduction in expression (Fig. 5). Both reduction of c-Myb expression and foci formation in telomeric DNA occurred in GBM spheres but not in non-GSCs following telomestatin treatment. Together, two distinct mechanisms of telomestatin action in GBM include, but may not be exclusive to, the direct disruption of telomere structure and inhibition of c-Myb.

In the CNS, c-Myb expression is restricted to the germinal zones of the adult brain and maintains progenitor cell proliferation and ependymal cell integrity (22). However, mice with the conditional brain-specific deletion of *c-Myb* exhibit only a mild defect in brain structure with hydrocephalus and ependymal cell abnormalities (22). To date, its function in gliomagenesis and maintenance of the immature state of GSCs has not been uncovered. We found that c-Myb expression is markedly elevated in clinical samples of GBM compared with normal brain tissues and undifferentiated GBM spheres compared with normal spheres or non-GSCs. Our functional data using knockdown and overexpression (Fig. 6) provide the first evidence that c-Myb plays a fundamental role in the growth of GSCs both *in vitro* and *in vivo*. Taken together, these data indicate that *c-Myb* is a potential new therapeutic target in the treatment of GBMs.

Telomestatin is a hydrophobic agent with a relatively large molecular weight (molecular weight = 583 kDa). The pharmacokinetics of this compound is not well defined and, more importantly, it is still unknown whether telomestatin penetrates the blood–brain barrier. In this study, we sought to use local (intratumoral) injection of telomestatin to deliver the drug directly to tumor cells. One of our aims is to identify safe and effective anti-GBM agents that can be applied to the removal cavity after tumor resection during surgery. Given that GBM is a tumor with an aggressive infiltrating nature, migrated tumor cells into the adjacent normal brain tissue are left behind during surgery. The presence of residual tumor cells makes relapse of the tumor inevitable within months or years of the surgery, despite adjuvant therapies. To achieve selective and effective eradication of the remaining tumor cells with minimal organ toxicity, we sought to identify anti-GSC agents that can be directly injected into the tumor cavity. Despite our positive data (Fig. 2), several open questions still remain. For instance, we cannot completely exclude the possibility of normal cell death

following local injection of telomestatin. Particularly, its effect on long-term self-renewal of normal NSCs in the subventricular zone and hippocampus in the adult brain needs to be fully addressed.

In this study, we showed that telomestatin treatment preferentially targets GBM cells with stem cell–like characteristics. Telomestatin decreased sphere-forming potential *in vitro*, reduced CD133-positive cell population *in vitro*, and decreased tumor sizes *in vivo*. In addition, normal neural precursors treated with the same dose of telomestatin showed less cytotoxicity. A search for target genes of telomestatin by cDNA microarray identified the proto-oncogene *c-Myb* and further functional analysis using GBM spheres showed that c-Myb plays a critical role in the growth of GSCs both *in vitro* and *in vivo*. Finally, a significant elevation of c-Myb expression in surgical specimens of GBM supports the clinical relevance of our findings. We believe that these data serve as a rationale for the design of a novel anti-GBM therapy. Future studies will shed light on the molecular functional role of c-Myb in GBMs and the therapeutic window of telomestatin for GBMs.

Translational Relevance

In this article, we addressed our hypothesis that a G-quadruplex ligand telomestatin eradicates glioma stem cells (GSC). For the majority of our assays, we used the patient-derived glioblastoma cells grown as spheres that are enriched with GSCs. Telomestatin treatment of these cultures, as well as the glioblastoma sphere–derived mouse xenograft tumor models, resulted in growth suppression and induction of apoptosis of GSCs. Furthermore, we showed that telomestatin has a novel target molecule, a proto-oncogene *c-Myb*. *c-Myb* was identified with the cDNA microarray experiments with telomestatin-treated cells, and pharmacodynamic analysis with the mouse model of glioblastoma confirmed the microarray results. Depletion of *c-Myb* by gene knockdown significantly reduced the growth of GSCs both *in vitro* and *in vivo*. Finally, immunohistochemistry of c-Myb with 90 clinical samples revealed a statistically significant elevation of c-Myb expression in surgical specimens of glioblastoma, supporting the significance of this proto-oncogene in glioblastoma biology.

Supplementary Material

Refer to Web version on PubMed Central for supplementary material.

Acknowledgments

The authors thank E.A. Chiocca (OSU), C.H. Kwon (OSU), J.N. Rich (Cleveland Clinic), P.J. Houghton (Nationwide Children’s Hospital), P.S. Mischel (UCLA), and H.I. Kornblum (UCLA) for discussions and comments, help with materials, and constructive criticisms. They also thank Mr. Anthony Harrington for the expert editorial assistance.

Grant Support

This work was supported by the start-up fund from the OSU, the Department of Neurological Surgery, and the Khan Family Foundation.

References

1. Vescovi AL, Galli R, Reynolds BA. Brain tumour stem cells. Nat Rev Cancer. 2006; 6:425–436. [PubMed: 16723989]
2. Cheng L, Bao S, Rich JN. Potential therapeutic implications of cancer stem cells in glioblastoma. Biochem Pharmacol. 2010; 80:654–665. [PubMed: 20457135]

3. Kim MY, Vankayalapati H, Shin-Ya K, Wierzba K, Hurley LH. Telomestatin, a potent telomerase inhibitor that interacts quite specifically with the human telomeric intramolecular g-quadruplex. J Am Chem Soc. 2002; 124:2098–2099. [PubMed: 11878947]
4. d'Adda di Fagagna F, Reaper PM, Clay-Farrace L, Fiegler H, Carr P, Von Zglinicki T, et al. A DNA damage checkpoint response in telomere-initiated senescence. Nature. 2003; 426:194–198. [PubMed: 14608368]
5. Counter CM, Avilion AA, LeFeuvre CE, Stewart NG, Greider CW, Harley CB, et al. Telomere shortening associated with chromosome instability is arrested in immortal cells which express telomerase activity. EMBO J. 1992; 11:1921–1929. [PubMed: 1582420]
6. Shin-ya K, Wierzba K, Matsuo K, Ohtani T, Yamada Y, Furihata K, et al. Telomestatin, a novel telomerase inhibitor from *Streptomyces anulatus*. J Am Chem Soc. 2001; 123:1262–1263. [PubMed: 11456694]
7. Gomez D, Paterski R, Lemarteleur T, Shin-Ya K, Mergny JL, Riou JF. Interaction of telomestatin with the telomeric single-strand overhang. J Biol Chem. 2004; 279:41487–41494. [PubMed: 15277522]
8. Guo K, Pourpak A, Beetz-Rogers K, Gokhale V, Sun D, Hurley LH. Formation of pseudosymmetrical G-quadruplex and i-motif structures in the proximal promoter region of the RET oncogene. J Am Chem Soc. 2007; 129:10220–10228. [PubMed: 17672459]
9. Qin Y, Fortin JS, Tye D, Gleason-Guzman M, Brooks TA, Hurley LH. Molecular cloning of the human platelet-derived growth factor receptor beta (PDGFR-beta) promoter and drug targeting of the G-quadruplex-forming region to repress PDGFR-beta expression. Biochemistry. 2010; 49:4208–4219. [PubMed: 20377208]
10. Lemarteleur T, Gomez D, Paterski R, Mandine E, Mailliet P, Riou JF. Stabilization of the c-myc gene promoter quadruplex by specific ligands' inhibitors of telomerase. Biochem Biophys Res Commun. 2004; 323:802–808. [PubMed: 15381071]
11. De Armond R, Wood S, Sun D, Hurley LH, Ebbinghaus SW. Evidence for the presence of a guanine quadruplex forming region within a polypurine tract of the hypoxia inducible factor 1alpha promoter. Biochemistry. 2005; 44:16341–16350. [PubMed: 16331995]
12. Huppert JL, Balasubramanian S. G-quadruplexes in promoters throughout the human genome. Nucleic Acids Res. 2007; 35:406–413. [PubMed: 17169996]
13. Tauchi T, Shin-Ya K, Sashida G, Sumi M, Nakajima A, Shimamoto T. Activity of a novel G-quadruplex-interactive telomerase inhibitor, telomestatin (SOT-095), against human leukemia cells: involvement of ATM-dependent DNA damage response pathways. Oncogene. 2003; 22:5338–5347. [PubMed: 12917635]
14. Tahara H, Shin-Ya K, Seimiya H, Yamada H, Tsuruo T, Ide T. G-Quadruplex stabilization by telomestatin induces TRF2 protein dissociation from telomeres and anaphase bridge formation accompanied by loss of the 3′ telomeric overhang in cancer cells. Oncogene. 2006; 25:1955–1966. [PubMed: 16302000]
15. Hemmati HD, Nakano I, Lazareff JA, Masterman-Smith M, Geschwind DH, Bronner-Fraser M, et al. Cancerous stem cells can arise from pediatric brain tumors. Proc Natl Acad Sci U S A. 2003; 100:15178–15183. [PubMed: 14645703]
16. Nakano I, Masterman-Smith M, Saigusa K, Paucar AA, Horvath S, Shoemaker L, et al. Maternal embryonic leucine zipper kinase is a key regulator of the proliferation of malignant brain tumors, including brain tumor stem cells. J Neurosci Res. 2008; 86:48–60. [PubMed: 17722061]
17. Visnyei K, Onodera H, Damoiseaux R, Saigusa K, Petrosyan S, De Vries D, et al. A molecular screening approach to identify and characterize inhibitors of glioblastoma stem cells. Mol Cancer Ther. 2011; 10:1818–1828. [PubMed: 21859839]
18. Nakano I, Joshi K, Visnyei K, Hu B, Watanabe M, Lam D, et al. Siomycin A targets brain tumor stem cells partially through a MELK-mediated pathway. Neuro Oncol. 2011; 6:622–634. [PubMed: 21558073]
19. Nakano I, Paucar AA, Bajpai R, Dougherty JD, Zewail A, Kelly TK, et al. Maternal embryonic leucine zipper kinase (MELK) regulates multipotent neural progenitor proliferation. J Cell Biol. 2005; 170:413–427. [PubMed: 16061694]

20. Nakano I, Dougherty JD, Kim K, Klement I, Geschwind DH, Kornblum HI. Phosphoserine phosphatase is expressed in the neural stem cell niche and regulates neural stem and progenitor cell proliferation. Stem Cells. 2007; 25:1975–1984. [PubMed: 17495110]
21. Viapiano MS, Hockfield S, Matthews RT. BEHAB/brevican requires ADAMTS-mediated proteolytic cleavage to promote glioma invasion. J Neurooncol. 2008; 88:261–272. [PubMed: 18398576]
22. Malaterre J, Mantamadiotis T, Dworkin S, Lightowler S, Yang Q, Ransome MI, et al. c-Myb is required for neural progenitor cell proliferation and maintenance of the neural stem cell niche in adult brain. Stem Cells. 2008; 26:173–181. [PubMed: 17901403]
23. Yaguchi S, Fukui Y, Koshimizu I, Yoshimi H, Matsuno T, Gouda H, et al. Antitumor activity of ZSTK474, a new phosphatidylinositol 3-kinase inhibitor. J Natl Cancer Inst. 2006; 98:545–556. [PubMed: 16622124]
24. Singh SK, Clarke ID, Terasaki M, Bonn VE, Hawkins C, Squire J, et al. Identification of a cancer stem cell in human brain tumors. Cancer Res. 2003; 63:5821–5828. [PubMed: 14522905]
25. Galli R, Binda E, Orfanelli U, Cipelletti B, Gritti A, De Vitis S, et al. Isolation and characterization of tumorigenic, stem-like neural precursors from human glioblastoma. Cancer Res. 2004; 64:7011–7021. [PubMed: 15466194]
26. Sonoda Y, Ozawa T, Hirose Y, Aldape KD, McMahon M, Berger MS, et al. Formation of intracranial tumors by genetically modified human astrocytes defines four pathways critical in the development of human anaplastic astrocytoma. Cancer Res. 2001; 61:4956–4960. [PubMed: 11431323]
27. Joo KM, Kim SY, Jin X, Song SY, Kong DS, Lee JI, et al. Clinical and biological implications of CD133-positive and CD133-negative cells in glioblastomas. Lab Invest. 2008; 88:808–815. [PubMed: 18560366]
28. Molofsky AV, Pardal R, Iwashita T, Park IK, Clarke MF, Morrison SJ. Bmi-1 dependence distinguishes neural stem cell self-renewal from progenitor proliferation. Nature. 2003; 425:962–967. [PubMed: 14574365]
29. Wakimoto H, Kesari S, Farrell CJ, Curry WT, Zaupa C, Aghi M, et al. Human glioblastoma-derived cancer stem cells: establishment of invasive glioma models and treatment with oncolytic herpes simplex virus vectors. Cancer Res. 2009; 69:3472–3481. [PubMed: 19351838]
30. Hu B, Kong LL, Matthews RT, Viapiano MS. The proteoglycan brevican binds to fibronectin after proteolytic cleavage and promotes glioma cell motility. J Biol Chem. 2008; 283:24848–24859. [PubMed: 18611854]
31. Shammas MA, Shmookler Reis RJ, Li C, Koley H, Hurley LH, Anderson KC, et al. Telomerase inhibition and cell growth arrest after telomestatin treatment in multiple myeloma. Clin Cancer Res. 2004; 10:770–776. [PubMed: 14760100]
32. Binz N, Shalaby T, Rivera P, Shin-ya K, Grotzer MA. Telomerase inhibition, telomere shortening, cell growth suppression and induction of apoptosis by telomestatin in childhood neuroblastoma cells. Eur J Cancer. 2005; 41:2873–2881. [PubMed: 16253503]
33. Gomez D, Wenner T, Brassart B, Douarre C, O'Donohue MF, El Khoury V, et al. Telomestatin-induced telomere uncapping is modulated by POT1 through G-overhang extension in HT1080 human tumor cells. J Biol Chem. 2006; 281:38721–38729. [PubMed: 17050546]
34. Muramatsu Y, Ohishi T, Sakamoto M, Tsuruo T, Seimiya H. Cross-species difference in telomeric function of tankyrase 1. Cancer Sci. 2007; 98:850–857. [PubMed: 17433040]
35. Takai H, Smogorzewska A, de Lange T. DNA damage foci at dysfunctional telomeres. Curr Biol. 2003; 13:1549–1556. [PubMed: 12956959]
36. Phillips HS, Kharbanda S, Chen R, Forrest WF, Soriano RH, Wu TD, et al. Molecular subclasses of high-grade glioma predict prognosis, delineate a pattern of disease progression, and resemble stages in neurogenesis. Cancer Cell. 2006; 9:157–173. [PubMed: 16530701]
37. Yi L, Zhou ZH, Ping YF, Chen JH, Yao XH, Feng H, et al. Isolation and characterization of stem cell-like precursor cells from primary human anaplastic oligoastrocytoma. Mod Pathol. 2007; 20:1061–1068. [PubMed: 17660801]
38. Son MJ, Woolard K, Nam DH, Lee J, Fine HA. SSEA-1 is an enrichment marker for tumor-initiating cells in human glioblastoma. Cell Stem Cell. 2009; 4:440–452. [PubMed: 19427293]

39. Palumbo SL, Memmott RM, Uribe DJ, Krotova-Khan Y, Hurley LH, Ebbinghaus SW. A novel G-quadruplex-forming GGA repeat region in the c-myb promoter is a critical regulator of promoter activity. Nucleic Acids Res. 2008; 36:1755–1769. [PubMed: 18252774]

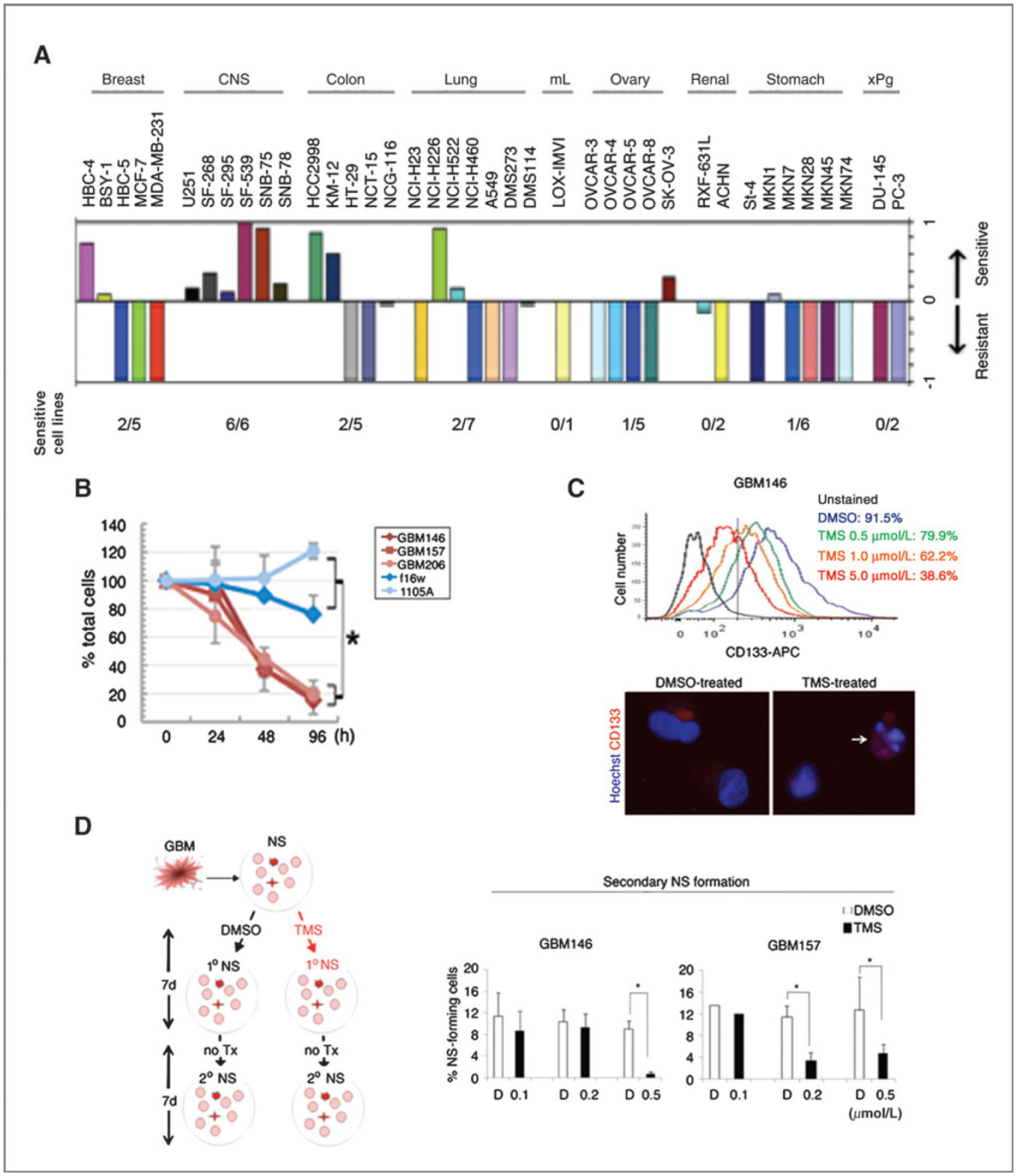

Figure 1.

Growth inhibition activity of telomestatin against GSCs. A, sensitivity of 39 cancer cell lines to telomestatin for 48 hours. A panel of 39 human cancer cell lines (termed JFCR39) was previously described (23). Values below zero indicate resistance to telomestatin, and values above zero indicate sensitivity. Negative (−) 1 indicates that the treatment with highest dose of telomestatin did not reach less than 50% decrease in cell number. B, time course of relative cell numbers of 3 GSC and 2 normal neural precursors at 1 μmol/L of telomestatin. *, statistical significance by two-sided *t* test ($P = 0.00049$). C, histograms indicating the proportions of CD133-positive cells in GBM146 spheres after treatment with

varying doses of telomestatin for 48 hours (top). Immunocytochemistry of GBM146 sphere cells stained with CD133 (red) after treatment with or without 1 μmol/L of telomestatin (TMS) for 48 hours (bottom). Hoechst dye was used for nuclear staining. The arrow indicates a CD133-positive cell with condensed fragmentation of nuclei. Original magnification, 40×. D, experimental flow (left). Graphs (right) indicate the proportions of sphere-forming cells derived from telomestatin (TMS)-pretreated 2 GBM samples (GBM146 and 157). APC, allophycocyanin; D, DMSO; mL, melanoma; NS, neurospheres. *, statistical significance by two-sided *t* test ($P < 0.05$).

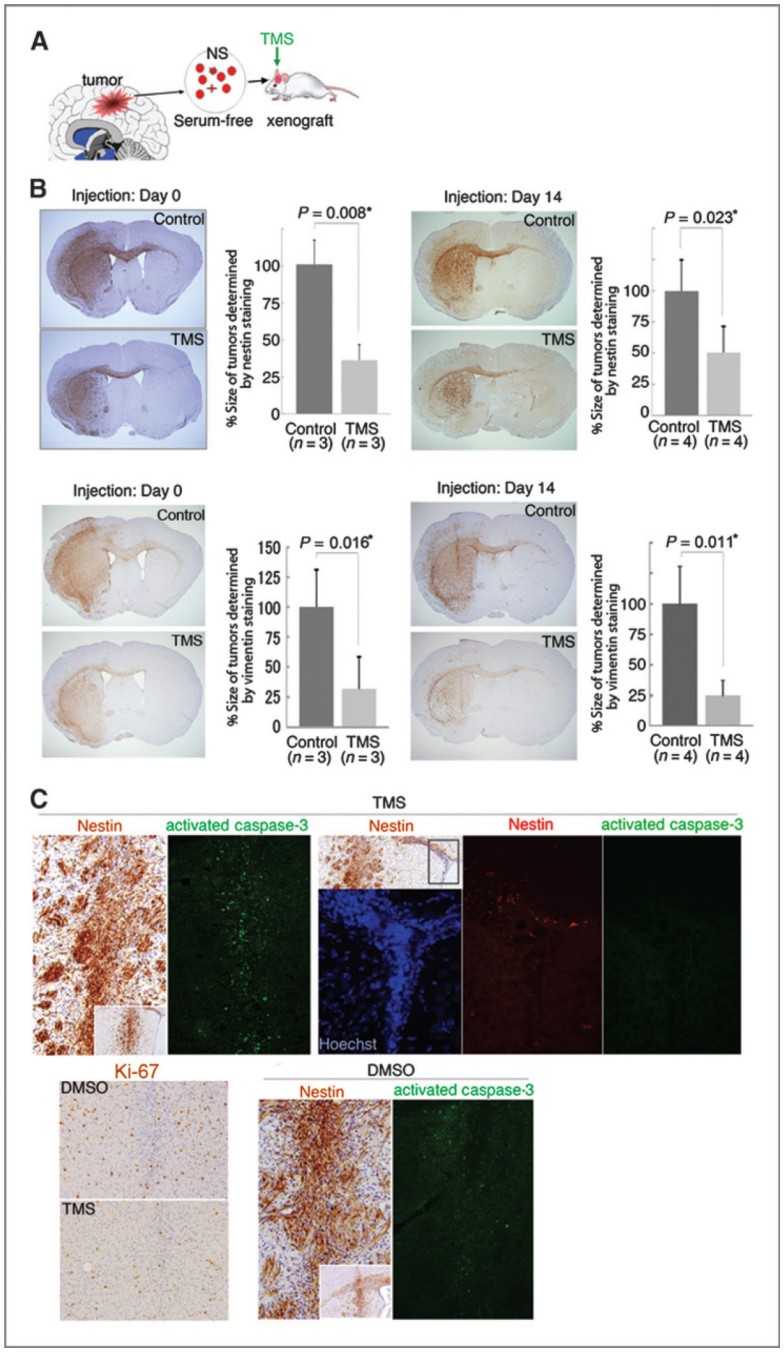

Figure 2.

Reduction of GSC-derived tumor sizes with intratumoral telomestatin (TMS) injection. A, experimental flow: telomestatin was injected into the tumor cavity by 2 different regimens, one with 5 pmol of telomestatin at the same time of tumor cell xenograft (day 0; left), the other with 50 pmol of telomestatin at 14 days after tumor cell xenograft (right). B, representative pictures indicate human-specific nestin staining (top) and vimentin staining (bottom) of immunocompromised mouse brains bearing GBM sphere–derived tumors with DMSO or telomestatin intratumoral injection at indicated time points. Original magnification, 2×. Graphs indicate the average of overall tumor sizes determined by immunostaining with human-specific antibody in each group. The number of mice in each

group is indicated in the graph. *, statistical significance by two-sided *t* test. Exact *P* values are indicated in the figure. C, immunohistochemistry of mouse brains at 2 days following intratumoral injection of DMSO or 2.5 nmol of telomestatin with antibodies for human-specific nestin, activated caspase-3, and Ki-67. Pictures at the injection site are shown in top left 2 panels and bottom panels and pictures at the lateral ventricle are shown in top right 3 panels. Original magnification, 20×.

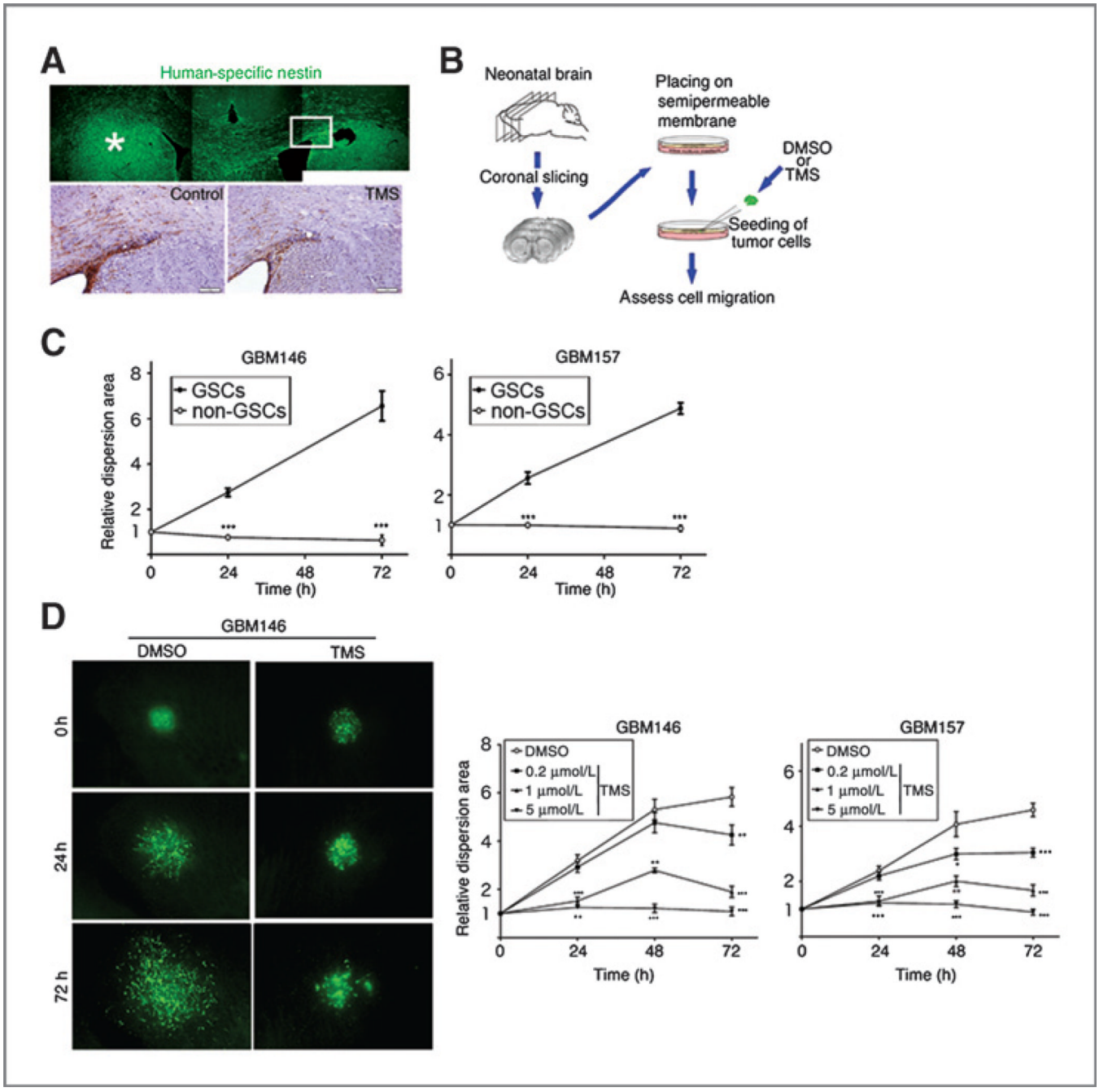

Figure 3.

Inhibitory effect of telomestatin (TMS) on GSC migration. A, representative pictures of human-specific nestin staining of immunocompromised mouse brains bearing human GBM157 sphere–derived tumors (top). Original magnification, 10×. *, location of xenograft. The rectangle indicates the region of magnification in the bottom. Human-specific nestin staining indicates migrated human GBM cells to the contralateral side of mouse brains through the corpus callosum in the control (DMSO-treated) group (bottom left) and telomestatin-treated group (bottom right). Original magnification, 40×. B, experimental flow for the migration assay in organotypic cultures of mouse brain slices. C, graphs for the time course of migration of GBM spheres (GSCs) and serum-propagated cells (non-GSCs)

derived from 2 GBM samples (GBM146 and 157). Quantitative analysis indicates cell dispersion (Area t_x/Area t_0). ***, statistical significance by 2-way ANOVA for repeated measures ($P < 0.001$). D, representative pictures of GFP-expressing human GBM146 cells dispersing on brain slices after treatment with 1 μmol/L of telomestatin or DMSO (left). Graphs indicate the relative dispersion of the cells normalized the initial size and fluorescence of the spheres (right). *, statistical significance by 2-way ANOVA for repeated measures (**, $P < 0.05$; ***, $P < 0.001$).

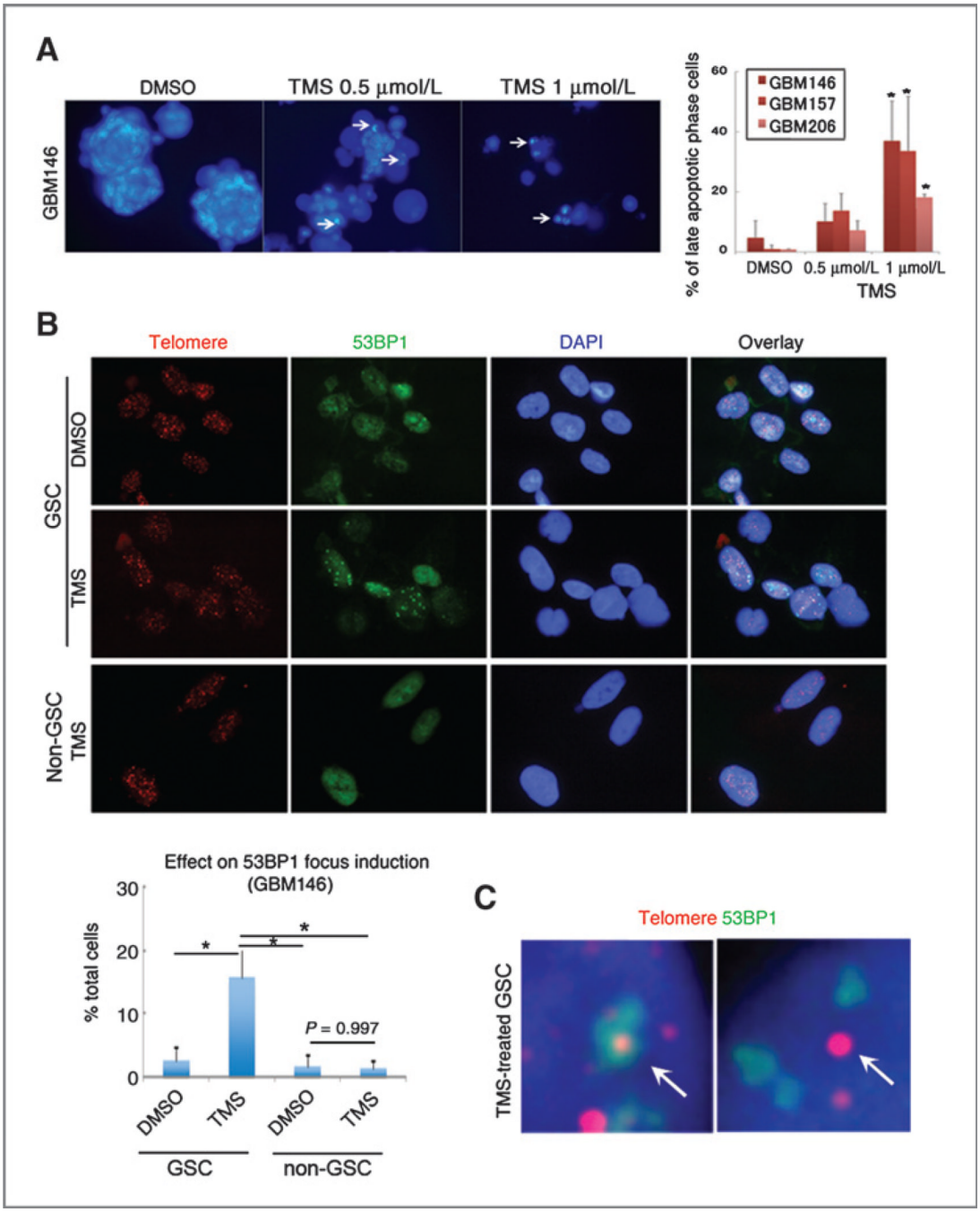

Figure 4.

Formation of 53BP1 foci in telomeric and non-telomeric DNA in GSCs, but not non-stem tumor cells. A, representative pictures of Hoechst dye staining to detect chromatin condensations in late apoptotic cells (indicated by arrows) treated with indicated dose of telomestatin (TMS) for 96 hours (left), and the graph indicating the proportion of apoptotic cells in 3 GBM spheres (right). *, statistical significance ($P < 0.05$). B, iFISH analysis indicating telomeric and non-telomeric DNA damages in telomestatin-treated GBM spheres. GBM146 spheres (GSCs) or serum-propagated GBM146 cells (non-GSCs) were treated with 1 µmol/L of telomestatin in serum-free medium for 96 hours and subjected to iFISH

analysis (top). Red, telomeric DNA; green, 53BP1; blue, DAPI staining for nuclear DNA. Quantitative graph of the 53BP1 focus–positive cells (bottom). GBM146 cells were classified into the focus-positive or -negative fractions according to the number of cells with punctate nuclear 53BP1 foci ($n > 2$). *, statistical significance ($P < 0.001$). C, magnified views of the representative telomere dysfunction–induced foci (arrow in left) and non-telomeric DNA damage foci (arrow in right) in GSCs derived from GBM146 treated with 1 μmol/L of telomestatin for 96 hours. DAPI, 40′, 6-diamidino-2-phenylindole.

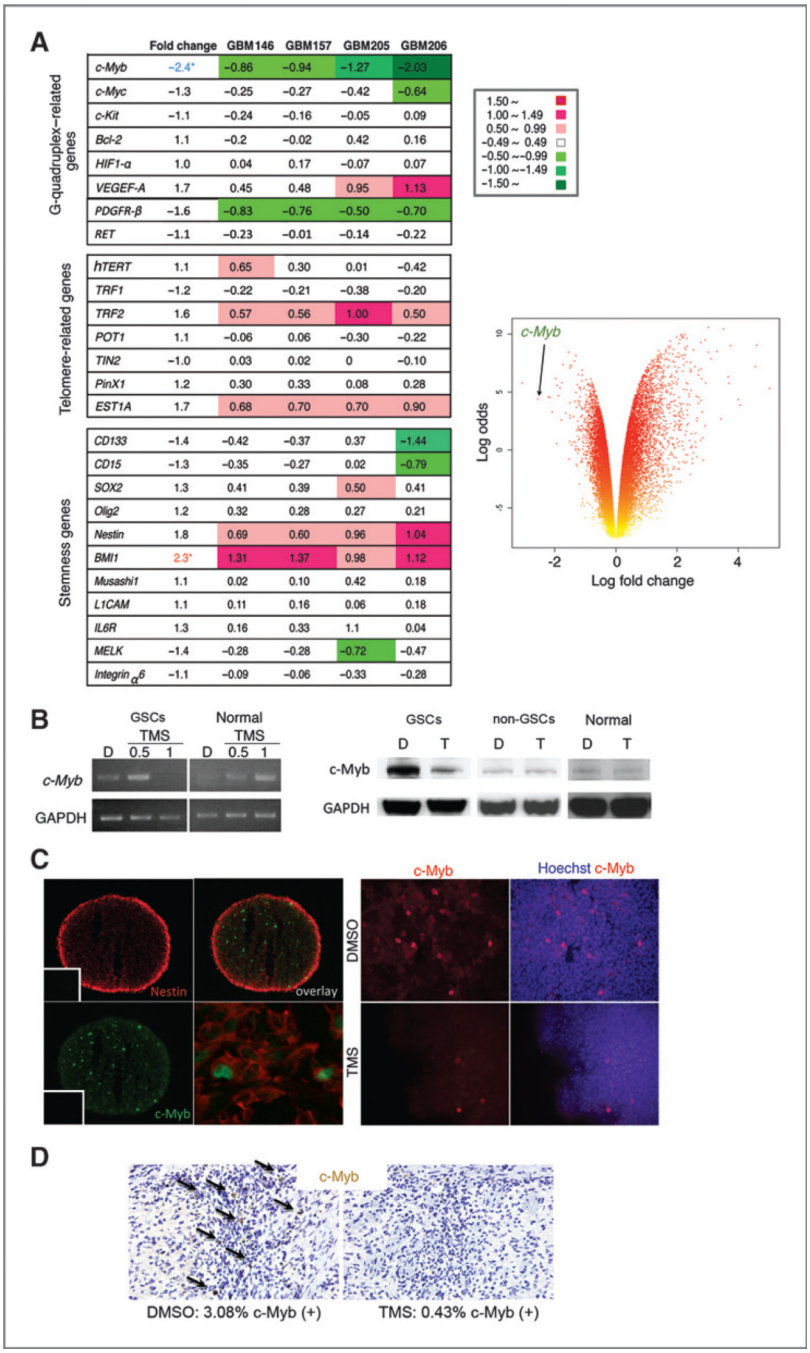

Figure 5.

c-Myb as a target of telomestatin (TMS) in GSCs. A, identification of distinct gene expression profiles in telomestatin-treated GSCs. The fold changes in representative candidates for indicated genes (left). Scatter plot of normalized signal intensities ofGSCs with telomestatin treatment (right). B, change of *c-Myb* expression level with telomestatin treatment in GBM146 spheres (GSCs), serum-propagated GBM146 cells (non-GSCs), and normal neural precursors (1105A) determined by RT-PCR and Western blot analysis D, DMSO; GAPDH, glyceraldehyde-3-phosphate dehydrogenase; T, telomestatin. C, immunocytochemistry of GBM157 spheres with c-Myb and human-specific nestin

antibodies. Hoechst is used for nuclear staining. Insets indicate staining results without the primary antibodies. Original magnification, 20×. D, pharmacodynamic analysis of telomestatin or DMSO on c-Myb expression in GBM157 sphere–derived tumors in mouse brains. Two days postinjection of telomestatin (2.5 nmol), brains were stained with c-Myb antibody and counterstained with hematoxylin. Arrows indicate c-Myb–positive cells at the injection site. The proportions of c-Myb–positive cells in total cells per field are indicated at the bottom.

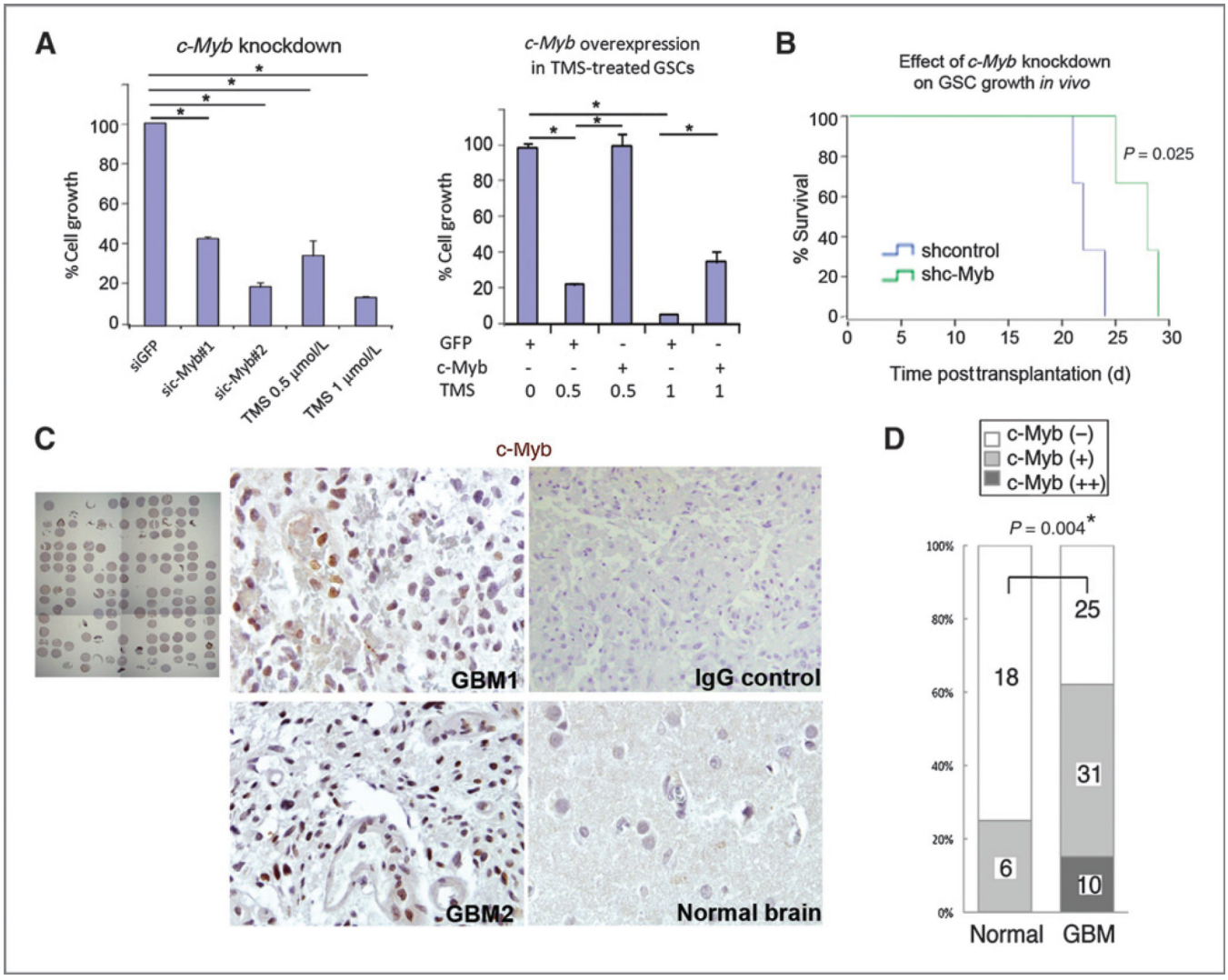

Figure 6.

c-Myb is essential for GSC growth and its expression is elevated in surgical specimens of GBMs. A, right graph indicates the relative cell numbers of GBM157 spheres at day 7 posttransfection with indicated siRNA constructs. Left graph indicates the relative cell numbers of GBM157 spheres at day 7 posttransfection with indicated vectors with or without telomestatin (TMS) treatment (*, $P < 0.001$). B, Kaplan–Meier curves indicating proportion of live mice harboring intracranial tumors derived from GBM13 spheres infected with short hairpin RNA (shRNA) lentivirus for *c-Myb* (sh*c-Myb*) or non-targeting sequence (shcontrol). C, a single slide with 66 GBM specimens and 24 normal brain tissues stained with c-Myb antibody (left). Representative staining results with 2 GBM tissues and one normal brain is shown (brown in middle). IgG control shows the background staining intensity. D, graph indicates the proportion of c-Myb strongly positive (++), weakly positive (+), and negative (−) samples in normal brain tissues ($n = 24$) and GBM tissues ($n = 66$; $P = 0.004$).